the observed plasma maximum concentrations and the time at which they occurred. This test failed to show any difference between the four tested forms with the two chosen parameters. Therefore, the study of the bioavailability of intramuscular, oral solution, tablet, and rectal suppository administration compared with intravenous administration showed that the intramuscular dosage form and oral tablets gave results similar to those obtained by intravenous injection, but the oral solution and the suppositories showed a mean lower bioavailability of 75 and 61%, respectively.

REFERENCES

(1) P. Casanova, *Hepatology*, **16**, 381 (1980).

(2) J. M. Segrestua, J. Gueris, D. Julien, and M. Tiar, *Thérapie*, **34**, 437 (1979).

(3) C. Laville and J. Margarit, *Sem. Hôp. Paris*, **58**, 323 (1982).

(4) E. Pommat, *Sem. Hôp. Paris*, **58**, 363 (1982).

(5) F. Battistelli and H. Lestradet, *Sem. Hôp. Paris*, **58**, 349 (1982).

(6) D. Girard, E. Salles, and A. Bel, *Sem. Hôp. Paris*, **58**, 353 (1982).

(7) G. Houin, F. Bree, N. Lerumeur, and J. P. Tillement, *J. Pharm. Sci.*, **72**, 71 (1983).

(8) W. J. Westlake, in "Principles and Perspectives in Drug Bioavailability," J. Blanchard, R. J. Sawchuk, and B. B. Brodie, Eds., Karger, Basel, 1979, chap. 1.

(9) P. D'Athis, M. O. Richard, D. Delauture, E. Rey, M. Bouvier-d'Yvoire, E. Clément, and G. Olive, *Thérapie*, **36**, 443 (1981).

(10) J. G. Wagner, in "Fundamentals of Clinical Pharmacokinetics," Drug Intelligence, Hamilton, Ill., 1975.

(11) W. G. Cochran and G. M. Cox, in "Experimental Designs," Wiley, New York, N.Y., 1957.

(12) W. J. Westlake, *Biometrics*, **30**, 319 (1974).

(13) W. J. Westlake, *Biometrics*, **32**, 741 (1976).

(14) D. D. Breimer, *J. Pharm. Sci.*, **64**, 1576 (1975).

(15) D. D. Breimer and A. G. de Boer, *Eur. J. Clin. Pharmacol.*, **9**, 169 (1975).

ACKNOWLEDGMENTS

We gratefully acknowledge Dr. Arunkumar Shastri for his critical revision of the manuscript.

Kinetic Study of the Polymorphic Transformations of Phenylbutazone

YOSHIHISA MATSUDA ˣ, ETSUKO TATSUMI, ETSUKO CHIBA, and YUKIE MIWA

Received June 15, 1983, from the *Kobe Women's College of Pharmacy, Higashinada, Kobe 658, Japan.* Accepted for publication December 5, 1983.

Abstract □ The polymorphic transformations of phenylbutazone from metastable forms α and β to stable form δ were studied quantitatively at four temperature and five humidity levels by X-ray powder diffractometry. The transformation of form α conformed with the Avrami-Erofe'ev kinetic model and form β conformed with apparent first-order kinetics. In the two transformation systems, the induction periods depended on the storage conditions and were prolonged with lowering of temperature and humidity. The transformation rate of form α was not affected by humidity, whereas that of form β increased according to a rise in humidity. The temperature dependency of the transformation rate constant was remarkable. The Arrhenius treatment was applicable to the $\beta \rightarrow \delta$ transformation at low temperatures. The overall half-life, including induction period, revealed that form α was more stable than form β under any storage condition. A good linear relationship existed between the induction period and the transformation rate constant, irrespective of the storage conditions. The scanning electron photomicrographs of forms α and β demonstrated that acicular crystals of form δ grew as the transformation progressed. This could be confirmed as the change in particle diameter of the samples.

Keyphrases □ Phenylbutazone—polymorphic transformation, physicochemical stability under different storage conditions □ Polymorphic transformation—phenylbutazone, physicochemical stability under different storage conditions □ Physicochemical stability—phenylbutazone, different storage conditions, polymorphic transformation

The method for improving the bioavailability of a slightly soluble drug is an important problem in the preformulation study of solid dosage forms. Polymorphic transformation is often effective as a technique for increasing solubility. Since the solubility and dissolution rate of a metastable polymorph are usually higher than those of the stable form, the former is more desirable clinically than the latter; however, the former is not always preferable in physicochemical stability. It is well known that, irrespective of temperature, only one crystal form is thermodynamically stable and all other forms convert eventually to the stable one. A metastable form nevertheless may occasionally exhibit sufficient stability to ensure a reasonable shelf life. If a metastable form is used in a formulation because of its excellent dissolution properties, it is prerequisite to demonstrate that the metastable form is never transformed to a more stable form under usual storage conditions.

Although some difficulties are involved in establishing a quantitative method for polymorphic transformation, there are several previous reports on the method (1–8). Due to the complexity of solid-state reaction, the stability-indicating kinetic interpretation has been fully discussed in only a few reports (1, 7, 8). The techniques described here are divided into three groups: IR spectrophotometry based on the quantitative Nujol mull technique (1–3, 6), differential scanning calorimetry (4, 5), and X-ray powder diffractometry (7, 8). Among these, X-ray diffractometry may be the most useful method because heat and liquid relating closely to polymorphic transformation are not involved in the measurement.

In the present investigation, the stability profiles between the two metastable forms of phenylbutazone are comparatively evaluated. The preparation and characterization of the phenylbutazone polymorphism have been described previously (9–16). The polymorphic system has been reported to consist of a stable form (form δ), four metastable forms (forms α, β, γ, and ϵ), and two pseudopolymorphs, among which form ϵ has the highest solubility. For the reasons of high yield and simplicity of preparation, forms α and β were chosen as polymorphic models in this study. The transformations of these forms were measured quantitatively by X-ray powder diffractometry and thoroughly studied over long periods of time under different storage conditions.

0022-3549/84/1000-1453$01.00/0

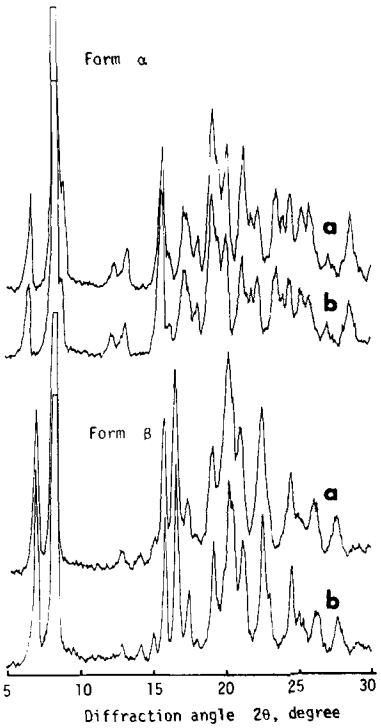

Figure 1—*X-ray diffraction patterns of forms α and β before and after milling. Key: (a) before milling; (b) after milling.*

EXPERIMENTAL SECTION

Preparation and Characterization of Polymorphs—*Form δ*—A single batch of commercial phenylbutazone[1] was used as received. The drug was confirmed to be form δ by X-ray powder diffraction analysis, differential scanning calorimetry (DSC), and IR spectroscopy.

Form α—An acetone solution (20% w/v) of the drug was evaporated to dryness under reduced pressure at 0°C by using a rotary evaporator.

Form β—The same solution as that used for form α was poured into 10 volumes of distilled water and stirred vigorously at room temperature. The separated crystals were removed by filtration through a sintered-glass funnel and dried under reduced pressure. These modifications were also characterized as forms α and β, respectively, according to a previously described method (16).

To expose the maximum surface area to ambient moisture, all modifications were micronized with a pin mill[2] at 26,960 rpm. The specific surface area diameters of the milled forms α and β, measured by an air permeability method (17), were 3.2 and 2.8 μm, respectively. The particle densities of forms α, β, and δ were determined with an air comparison pycnometer[3]. The X-ray powder diffraction patterns and the DSC data of the samples before and after milling indicated that no polymorphic transformation occurred during the milling operation (Figs. 1 and 2).

Determination of Transformation Rate—*Preparation of Calibration Curves by X-ray Powder Diffractometry*—Known quantities of form α or β were thoroughly mixed with form δ in various proportions in a mortar. The mixtures (250 mg each) were subjected to X-ray powder diffraction analysis. The X-ray diffraction pattern was recorded according to a previously described method (16). The instrument was set as follows: (*a*) 35 kV, 7 mA; (*b*) 1° beam slit and 0.2° detector slit; (*c*) count range, 1000 cps; (*d*) time constant, 1 s; (*e*) range of diffraction angle 2θ = 30–5°; (*f*) scanning speed, 4°/min; and (*g*) chart speed, 40 mm/min.

Although the X-ray diffraction pattern of form δ obviously differed from that of forms α and β (16), most of the peaks characterized by these forms in the mixture were not fully separated due to the close vicinity of the diffraction angles. Figure 3 represents the typical X-ray diffraction patterns of various proportions for α–δ and β–δ binary mixtures by weight basis. The changes in peaks (arrows) accompanying various mixing ratios were especially remarkable at the diffraction angles of 6.6°, 7.1°, 19.1°, and 20.1° for the α–δ system and at 15.6°, 16.4°, 20.1°, and 21.0° for the β–δ system. These

[1] Ciba-Geigy (Japan) Ltd.
[2] Contraplex-Labormühle 63C; Alpine AG, Federal Republic of Germany.
[3] Model 930; Beckman-Toshiba Co. Ltd., Tokyo, Japan.

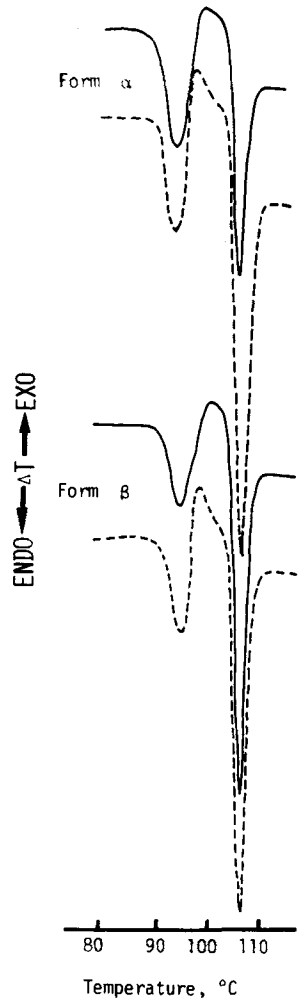

Figure 2—*DSC curves for forms α and β before (—) and after (- - -) milling. Sample weights: 7.30, 9.21, 8.19, and 8.01 mg (from top to bottom); heating rate, 10°C/min; sensitivity, ±20 mJ/s.*

peaks consisted of the individual peak characterizing each form. Thus, the diffraction intensity ratios of the two adjacent diffraction angles were plotted against the weight fraction of each component (Fig. 4). Despite the fluctuation of the individual diffraction intensity, these plots were always reproducible to give a smooth curve for any of the mixing ratios. Since curve a (Fig. 4) for the α–δ system approached infinity at the lower weight fraction of form δ, the reciprocal values of intensity ratios were regressed with curve b (Fig. 4), and their terminal regions were made up for each other (thick line of the left panel, Fig. 4). Although the calibration data for the α–δ and β–δ systems could be obtained as straight lines on the middle part of log-probability and semi-logarithmic scales, respectively, they deviated from these lines on the terminal regions. Therefore, the original calibration curves were used. The conversion rates for the two systems were expressed by the mean of values estimated from the two calibration curves.

The changes in diffraction intensity at these angles are shown for the actual transformation system in Fig. 5. The time course change in relative diffraction intensity was clearly observed, indicating the validity of this method.

Preparation of Calibration Curves by Differential Scanning Calorimetry—For purposes of comparison with the X-ray powder diffractometry method, DSC was employed for determining the conversion rate. Similarly to X-ray powder diffractometry, preparation of an exactly equal amount of mixed samples of varying weight ratios was attempted to accomplish the plotting of DSC data. This was almost impossible from a technical point of view; therefore, the following method was alternatively employed. Different amounts of form α or β were accurately weighed and thermograms of these pure samples were recorded in a closed pan system. The DSC[4] operation conditions were: (*a*) heating rate, 5°C/min; (*b*) sensitivity, ±5 mJ/s; (*c*) chart speed, 40 mm/min; (*d*) flow rate of nitrogen gas, 30 mL/min. Forms α and β exhibited endothermic peaks at 91.0–92.0°C and 95.0–96.5°C, respectively,

[4] DSC-30; Shimadzu Co., Kyoto, Japan.

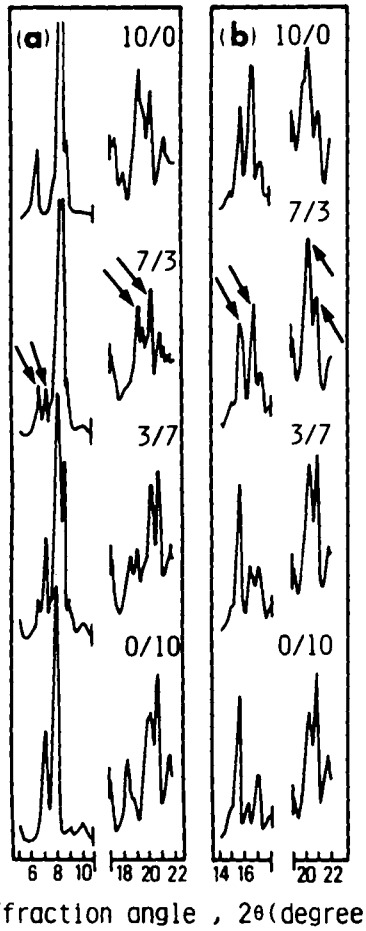

Figure 3—*X-ray diffraction patterns of α–δ and β–δ binary mixtures in various ratios. Key: (a) α–δ system; (b) β–δ system. The fraction in the graph represents the form α (form β)/form δ weight ratio.*

which subsequently underwent polymorphic transformations to show exothermic peaks at 93.0–94.0°C and 96.5–98.0°C, respectively. Two areas consisting of an area surrounded by both an endothermic peak curve and a line connecting the starting point of the endothermic peak with the top of the exothermic peak and another area surrounded by the same curve and the line connecting the same point with the terminal point of the exothermic peak were regarded as areas A and B, respectively (Fig. 6). The areas were measured by a gravimetric technique and were plotted against sample weight. Good straight lines were obtained between both parameters for the two systems. The conversion rate was expressed as the ratio of the mean of the two values estimated with lines A and B to the weight of sample on an aluminum pan.

Storage Conditions and Sampling of Polymorphs—About 1.2 g of a sample was placed in a vial as lightly as possible and stored over saturated solutions of various salts placed in laboratory desiccators. The desiccators were kept in a thermostated cabinet. The samples for thermal analysis were placed on an aluminum pan and stored in the same desiccators. The temperatures and humidities used were 25, 40, 50, and 60°C and 0, 30, 50, 70, and 80% relative humidity, respectively. Phosphorus pentoxide was used to provide a limiting humidity of 0% relative humidity at 60°C. The stored sample was withdrawn from each vial at various time intervals for X-ray powder diffractometry. After the measurement, the sample was returned to the vial for further storage.

Scanning Electron Microscopy—The scanning electron photomicrographs of the samples stored at 60°C and 80% relative humidity were taken with a microscope[5] at magnifications ranging from 600× to 2000×.

RESULTS AND DISCUSSION

Kinetic Interpretation of Transformation Processes—Since the solid-state reaction is essentially a surface phenomenon, the solid–solid transformation of a metastable polymorph may require a long period of time under mild stress condition. The residual percentage was determined by the X-ray powder

[5] Model JSM-U3; JEOL Co. Ltd., Tokyo, Japan.

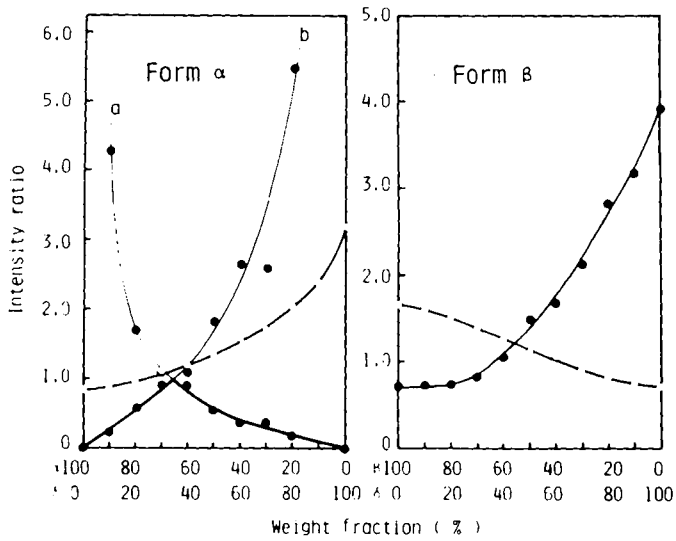

Figure 4—*Calibration curves for forms α and β by X-ray diffractometry Key: (intensity ratio for form α) (○) 20.1°/19.1°; (●) 6.6°/7.1° (a) or 7.1°/6.6° (b); (intensity ratio for form β) (○) 20.1°/21.0°; (●) 15.6°/16.4°.*

diffraction method (Fig. 7). The typical transformation profiles of the forms obtained under the extreme stress condition of 60°C are illustrated. Form β underwent transformation more rapidly than form α at any humidity. A distinct difference on the pattern of curves was seen between forms α and β, suggesting a different mechanism of transformation; the best-fitting curves

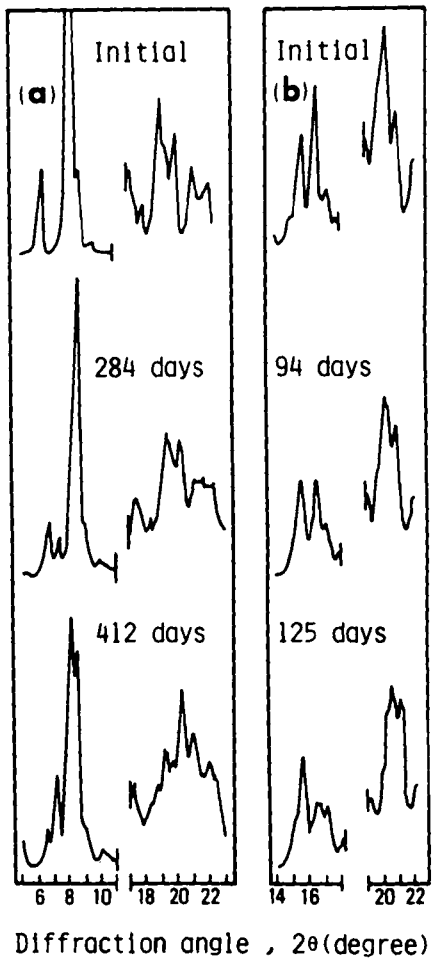

Figure 5—*Changes in X-ray diffraction intensities of forms α and β under polymorphic transformations. Key: (a) α → δ transformation at 40°C and 80% relative humidity. (b) β → δ transformation at 40°C and 30% relative humidity. The number in the graph represents the number of days after storage was begun.*

Table I—Values of m^a for $\alpha \rightarrow \delta$ and $\beta \rightarrow \delta$ Polymorphic Transformation Rate Equations

Transformation System	Temperature, °C	Relative Humidity, %				
		0	30	50	70	80
$\alpha \rightarrow \delta$	25	—[b]	NC[c]	NC	NC	NC
	40	—	NC	NC	2.10	1.93
	50	—	1.91	1.98	1.93	1.76
	60	1.57[d]	—	1.99	2.04	1.89
$\beta \rightarrow \delta$	25	—	0.98	1.03	0.88	1.01
	40	—	0.94	0.84	0.99	0.89
	50	—	1.00	1.01	0.98	0.96
	60	1.02	—	1.02	0.82	0.98

[a] See Eq. 2. [b] Experiment was not carried out. [c] Not calculated; m value could not be calculated because the transformation did not proceed at all or proceeded only to a small extent. [d] Few data were available.

Table II—Correlation Coefficients for the m Values in Table I

Transformation System	Temperature, °C	Relative Humidity, %				
		0	30	50	70	80
$\alpha \rightarrow \delta$	25	—[a]	NC[b]	NC	NC	NC
	40	—	NC	NC	0.952 (6)[c]	0.994 (7)
	50	—	0.998 (5)	0.995 (9)	0.994 (8)	0.998 (8)
	60	1.000 (4)	—	0.987 (6)	0.996 (6)	0.998 (6)
$\beta \rightarrow \delta$	25	—	0.968 (10)	0.986 (10)	0.940 (5)	0.991 (10)
	40	—	0.772 (5)	0.999 (4)	0.990 (5)	0.995 (6)
	50	—	1.000 (5)	0.991 (7)	0.994 (5)	1.000 (5)
	60	0.988 (7)	—	1.000 (4)	0.990 (4)	0.999 (4)

[a] Experiment was not carried out. [b] Not calculated; coefficient of correlation could not be calculated because the transformation did not proceed at all or proceeded only to a small extent. [c] Number of plots are indicated in parentheses.

for form α were all sigmoidal in shape, whereas those for form β were exponential. Similar profiles were obtained for the samples stored under other conditions of temperature and humidity. A common feature was the presence of an induction period similar to that obtained by Moustafa *et al.* (1, 2), which varied depending on the storage condition.

Figure 8 shows the comparison of the residual percentage determined by X-ray diffractometry with that determined by the DSC for the same sample as shown in Fig. 7. Irrespective of the humidity level, a good correspondence was obtained after the middle stage of the $\alpha \rightarrow \delta$ transformation. However, in the earlier stage of the $\alpha \rightarrow \delta$ transformation and throughout the entire process of $\beta \rightarrow \delta$ transformation, such a correspondence could not be established; the DSC resulted in an overestimation of the conversion rate. These results indicate that during the course of heating some further transformation occurred before the transition peak was observed. The DSC thus proved to be inadequate for determining the conversion rate in the present transformation systems; therefore, the subsequent determinations were carried out by the X-ray powder diffractometry method alone.

To confirm the conformance of isothermal kinetic data to theoretical kinetic equations, an interpretation method by Hancock and Sharp (18) was applied to the accompanying Avrami-Erofe'ev equation (19):

$$\ln [-\ln (1 - \alpha)] = m \cdot \ln t + \ln B \qquad \text{(Eq. 1)}$$

where α and t represent a conversion rate of polymorph and storage time, respectively, B is a constant, and m is the constant relating to the mechanism of transformation. In the present transformation systems, Eq. 1 should be modified as:

$$\ln [-\ln (1 - \alpha)] = m \cdot \ln (t - t_i) + \ln B \qquad \text{(Eq. 2)}$$

where t_i is the induction period. Equation 2 indicates that a linear relationship of a gradient m exists between the values of $-\ln (1 - \alpha)$ and $t - t_i$ on the double logarithmic scale. The best-fitting values for m and t_i, which should give the maximum coefficient of correlation, were calculated from the conversion rates to be <80% by the computer-aided least-squares method. The values for m and the correlation coefficients are given in Tables I and II, respectively.

Although several values were somewhat abnormal due to the paucity of data, the integer m values for $\alpha \rightarrow \delta$ and $\beta \rightarrow \delta$ transformations were rounded up to 2 and 1 from their mean values of 1.95 and 0.96, respectively. Equations 3 and 4 are, consequently, derived from Eq. 2:

$$[-\ln (1 - \alpha)]^{1/2} = k_1 (t - t_i) \; (\alpha \rightarrow \delta \text{ transformation}) \qquad \text{(Eq. 3)}$$

$$\ln (1 - \alpha) = -k_2 (t - t_i) \; (\beta \rightarrow \delta \text{ transformation}) \qquad \text{(Eq. 4)}$$

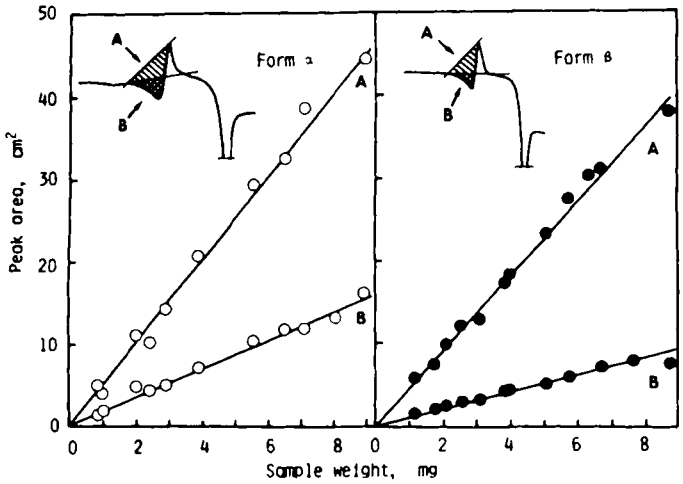

Figure 6—*Calibration curves for forms α and β by DSC. Key: (○) form α; (●) form β. The straight lines A and B indicate the areas A and B, respectively.*

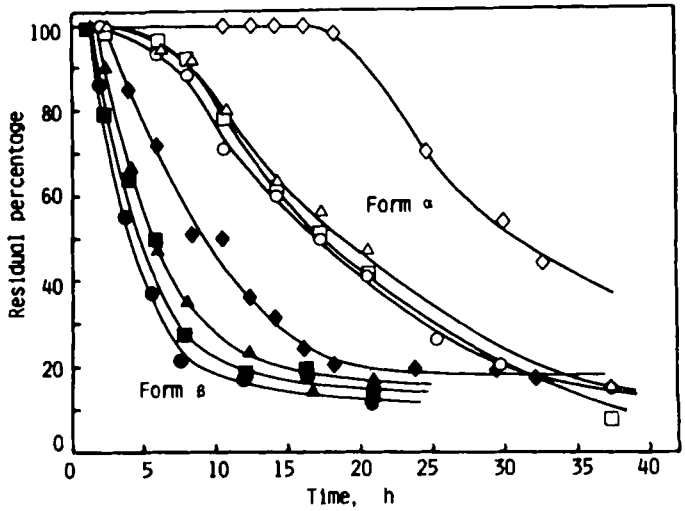

Figure 7—*Time course of $\alpha \rightarrow \delta$ and $\beta \rightarrow \delta$ transformations at 60°C. Key: (◇ ◆) 0%; (△ ▲) 50%; (□ ■) 70%; (○ ●) 80% relative humidity.*

Table III—Correlation Coefficients for Transformation Models[a]

Transformation System	Temperature °C	Relative Humidity, % 0	30	50	70	80
$\alpha \rightarrow \delta$	25	—[b]	NC[c]	NC	NC	NC
	40	—	NC	NC	0.960 (6)[d]	0.992 (7)
	50	—	0.981 (5)	0.995 (9)	0.994 (8)	0.994 (8)
	60	0.986 (4)	—[b]	0.987 (6)	0.993 (6)	0.997 (6)
$\beta \rightarrow \delta$	25	—	−0.969 (10)	−0.967 (10)	−0.966 (5)	−0.944 (10)
	40	—	−0.995 (5)	−0.993 (4)	−0.995 (5)	−0.991 (6)
	50	—	−0.994 (5)	−0.988 (7)	−0.993 (5)	−1.000 (5)
	60	−0.991 (7)	—	−0.999 (4)	−0.976 (4)	−0.998 (4)

[a] See Eqs. 3 and 4 in the text. [b] Experiment was not carried out. [c] Not calculated; coefficient of correlation could not be calculated because the transformation did not proceed at all or proceeded only to a small extent. [d] Number of plots are indicated in parentheses.

Table IV—Overall Half-Lives Under Different Storage Conditions (days)

Transformation System	Temperature °C	Relative Humidity, % 0	30	50	70	80
$\alpha \rightarrow \delta$	25	—[a]	NC[b]	NC	NC	NC
	40	—	NC	NC	411	346
	50	—	165	142	151	125
	60	1.28	—	0.79	0.74	0.74
$\beta \rightarrow \delta$	25	—	456	455	436	360
	40	—	100	98	79	70
	50	—	12.0	9.1	6.3	5.5
	60	0.40	—	0.24	0.21	0.18

[a] Experiment was not carried out. [b] Half-life could not be calculated because the transformation did not proceed at all or proceeded only to a small extent.

where k_1 and k_2 are transformation rate constants. The values for both transformation systems in Fig. 7 were plotted according to Eqs. 3 and 4 (Fig. 9). All values gave straight lines under all storage conditions; hence, the regression analyses were repeated by using Eqs. 3 and 4 to calculate the values of t_i, k_1, and k_2 (Table III).

The m value of 2 suggests that $\alpha \rightarrow \delta$ transformation is controlled by a nucleation-and-growth reaction and that the growth of the stable form may take place by a one- or two-dimensional mechanism (20). According to a reaction model (21) conforming to this kinetic expression (Eq. 3), which described the first formation followed by growth of potential nuclei on the surface of the drug, the nucleation was rapid and complete. Therefore, the growth appeared to be two-dimensional. On the contrary, the result of the $\beta \rightarrow \delta$ transformation conforming to the first-order kinetics suggests that the rate of transformation is controlled by random nucleation (*cf.* instantaneous nucleation for $\alpha \rightarrow \delta$ transformation) in an assemblage of an identical reactant fragment (21).

Effects of Temperature and Humidity on the Induction Period and Transformation Rate Constant—Since the induction period and transformation rate depend on the mobility of constituent atoms or molecules of the solid, they must vary considerably with temperature. The effects of temperature and humidity on the induction period on semilogarithmic scales are illustrated in Fig. 10, in which the relative humidity is converted to absolute humidity to provide a thorough understanding of the water contents. The right terminal point of each regression line represents the limiting absolute humidity corresponding to 100% relative humidity at the designated temperature. Temperature affected the induction period more markedly than did humidity. The two transformation systems showed a common tendency to prolong the induction period with a lowering in temperature and humidity, suggesting the delayed initiation of nucleation of the stable form. It should be emphasized that even under the extreme humidity condition of 0% relative humidity at 60°C the induction period was always a finite value for the two transformation systems. The micronization of samples by milling may cause generation of a large number of point defects or dislocations on the crystal surfaces, resulting in selective heterogeneous nucleation. Judging from the water-absorbing power of phosphorus pentoxide[6], as well as the environmental temperature and atmospheric pressure, complete desorption of water molecules on the sites of potential nuclei formation seems to be difficult under these conditions. Therefore, even though the amount of water is very small, it may serve as a nucleation catalyst.

Moustafa *et al.* (1) interpreted the induction period as the time required for equilibration of the crystal surfaces with water vapor. However, the results that the induction period was a finite value at 0% relative humidity and was prolonged at lower temperatures indicate reasonably that the induction period is defined as the time at which the embryo of a stable form grows to the critical nuclei at the nuclei formation sites.

Figure 11 illustrates the effects of temperature and humidity on the

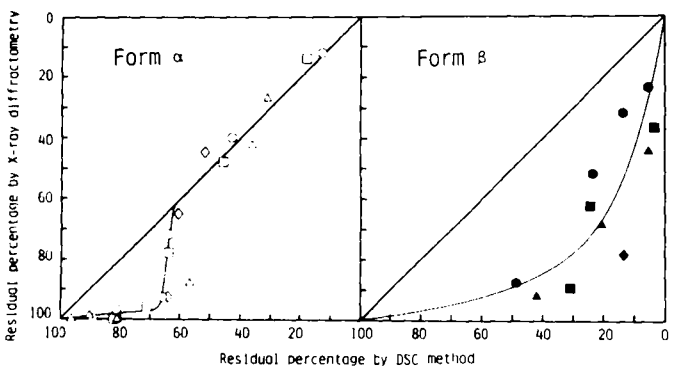

Figure 8—*Relationship between residual percentages of forms α and β at 60°C determined by X-ray diffractometry and those determined by differential scanning calorimetry. Key: (◇ ◆) 0%; (△ ▲) 50%; (□ ■) 70%; (○ ●) 80% relative humidity.*

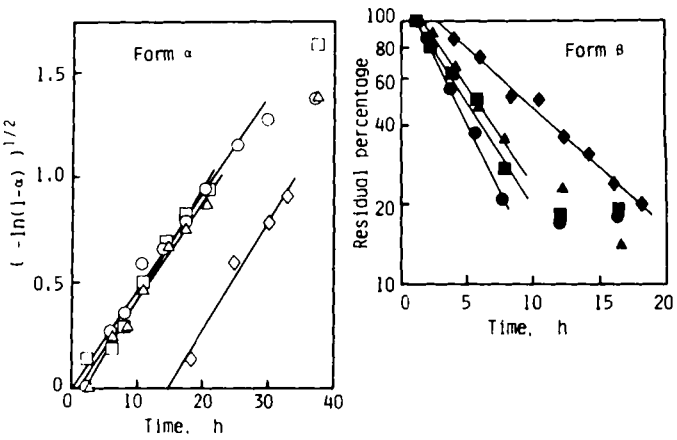

Figure 9—*Applicability of the Avrami-Erofe'ev (19) equation to α → δ transformation and of first-order kinetic model to β → δ transformation at 60°C (see Eqs. 3 and 4). Key: (◇ ◆) 0%; (△ ▲) 50%; (□ ■) 70%; (○ ●) 80% relative humidity.*

[6] The water content remaining in dried air over phosphorus pentoxide in a desiccator is 2.5×10^{-5} mg/L (*cf.* Ref. 22).

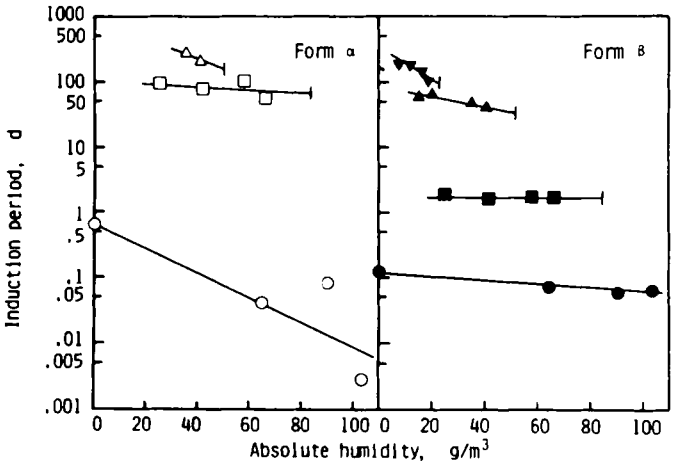

Figure 10—*Effect of absolute humidity on induction periods at different temperatures. Key: (▼) 25°C; (△▲) 40°C; (□■) 50°C; (○●) 60°C. The induction periods for α → δ transformation at 25°C could not be obtained within the time course of this investigation.*

transformation rate constant. The rate constants for forms α and β showed the same dimension of day^{-1}. It was, however, meaningless to use these values for comparison with the rate of transformation, because the mechanisms of transformation differed. The rate constant and the induction period were remarkably affected by temperature, and the rate was increased with a rise in temperature. The difference between the two transformations was distinct: the transformation of form α was not affected by humidity, whereas form β underwent transformation by a complex action of temperature and humidity. Furthermore, the higher the temperature, except for 60°C in the form β transformation, the stronger the dependence on humidity. These data indicate that storage at lower temperature and humidity is essential to inhibit polymorphic transformation.

The estimated half-life, including induction period, was much smaller in form β than in form α under any storage condition, indicating that form β is less stable (Table IV). The order of the thermodynamic instabilities of forms α and β corresponds well to that of superiority in dissolution properties (16).

Figure 12 shows the elevated temperature transformation data plotted by the Arrhenius procedure, in which the logarithmic values for the rate constants obtained by interpolating or extrapolating each regression line of Fig. 11 to the designated absolute humidity are plotted against the reciprocal of absolute temperature. Only one plot was obtainable at each temperature for form α, because the rate constant was not humidity dependent. The rate constant at 25°C was not obtained, because no transformation occurred within the time course of the present investigation. Good linear relationships existed for the β → δ transformation at lower humidities at temperature levels ranging from 25°C to 50°C, indicating that the higher the humidity, the steeper the slope

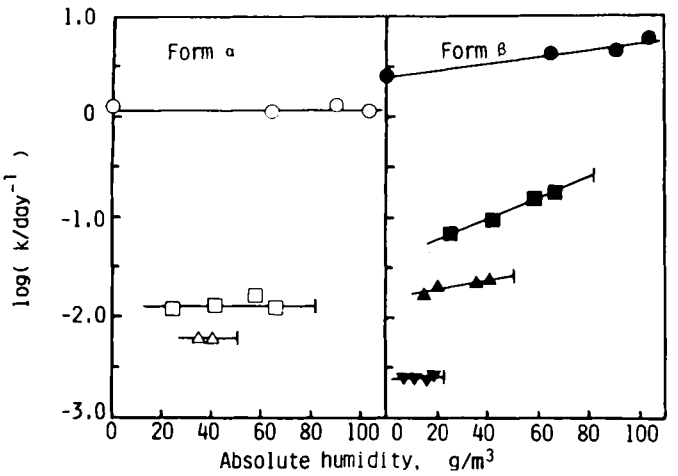

Figure 11—*Effect of absolute humidity on the transformation rate constant at different temperatures. Key: (▼) 25°C; (△▲) 40°C; (□■) 50°C; (○●) 60°C. The transformation rate constants for α → δ transformation at 25°C could not be obtained, because no transformation started within the time course of this investigation.*

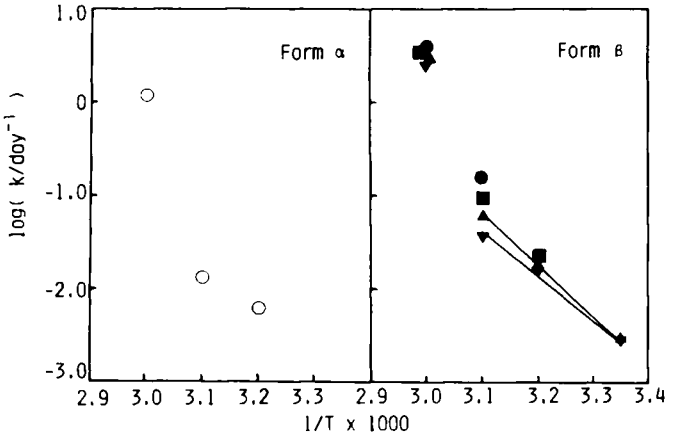

Figure 12—*Arrhenius plot for α → δ and β → δ transformations at different absolute humidities. Key: (○) 0, 20, 40, and 60 g/cm³ for α → δ transformation; (▼) 0 g/cm³, (▲) 20 g/cm³, (■) 40 g/cm³, (●) and 60 g/cm³ for β → δ transformation.*

of the straight line. Although the linearity and/or temperature dependency of the slope at higher humidities were blurry due to insufficient data, the activation energy for transformation was found to increase gradually with an increase in humidity. The dehydration processes from crystals entrapping water of crystallization were also affected by temperature and water vapor pressure (23, 24), *e.g.*, the activation energy for dehydration increases with a rise in water vapor pressure (24). However, the role of water in the present transformation systems fundamentally differed from that in the dehydration reaction. Since the transformation rate is a function of several variables possessing different temperature coefficients, this result is not easily explained.

The activation energies thus determined at absolute humidities of 0 and 20 g/m³ were ~21.7 and 25.1 kcal/mol, respectively. These values were much smaller than the activation energy of ~203 kcal/mol (11) that was determined by the method of Kissinger (25). Weaker intermolecular actions such as van der Waals forces or hydrogen bonds are predominant in polymorphs; therefore, the transformation must not require a higher activation energy. The validity of this suggestion may be supported by the facts that the activation energy for the polymorphic transformation in binaphthyl is ~60 kcal/mol and that for *p*-dichlorobenzene is much smaller (17 kcal/mol) (26). It is also interesting to note that the activation energy for loss of water from cytosine monohydrate is ~25 kcal/mol (26).

The rate constants at 60°C in the two transformation systems were abnormally higher than those estimated by extrapolating the regression lines, suggesting that the activation energies became high at ~60°C. Additional information on other transformation systems is needed to understand why a change in activation energy accompanies a rise in temperature. It has been reported that since not all solid-state reactions conform to the Arrhenius treatment, the activation energy is not necessarily constant with temperature (27, 28).

The kinetic behavior during the induction period and in the transformation rate constant suggest the close relationship between them. The double-logarithmic plotting of both factors gave a good straight line, irrespective of the storage conditions for the two transformation systems (Fig. 13). It was verified

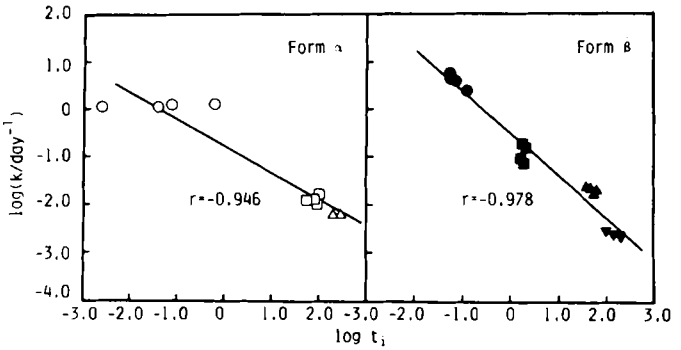

Figure 13—*Relationships between induction period and transformation rate constant for α → δ and β → δ transformations. Key: (▼) 25°C; (△▲) 40°C; (□■) 50°C; (○●) 60°C. The plots for α → δ transformation at 25°C could not be obtained within the time course of this investigation.*

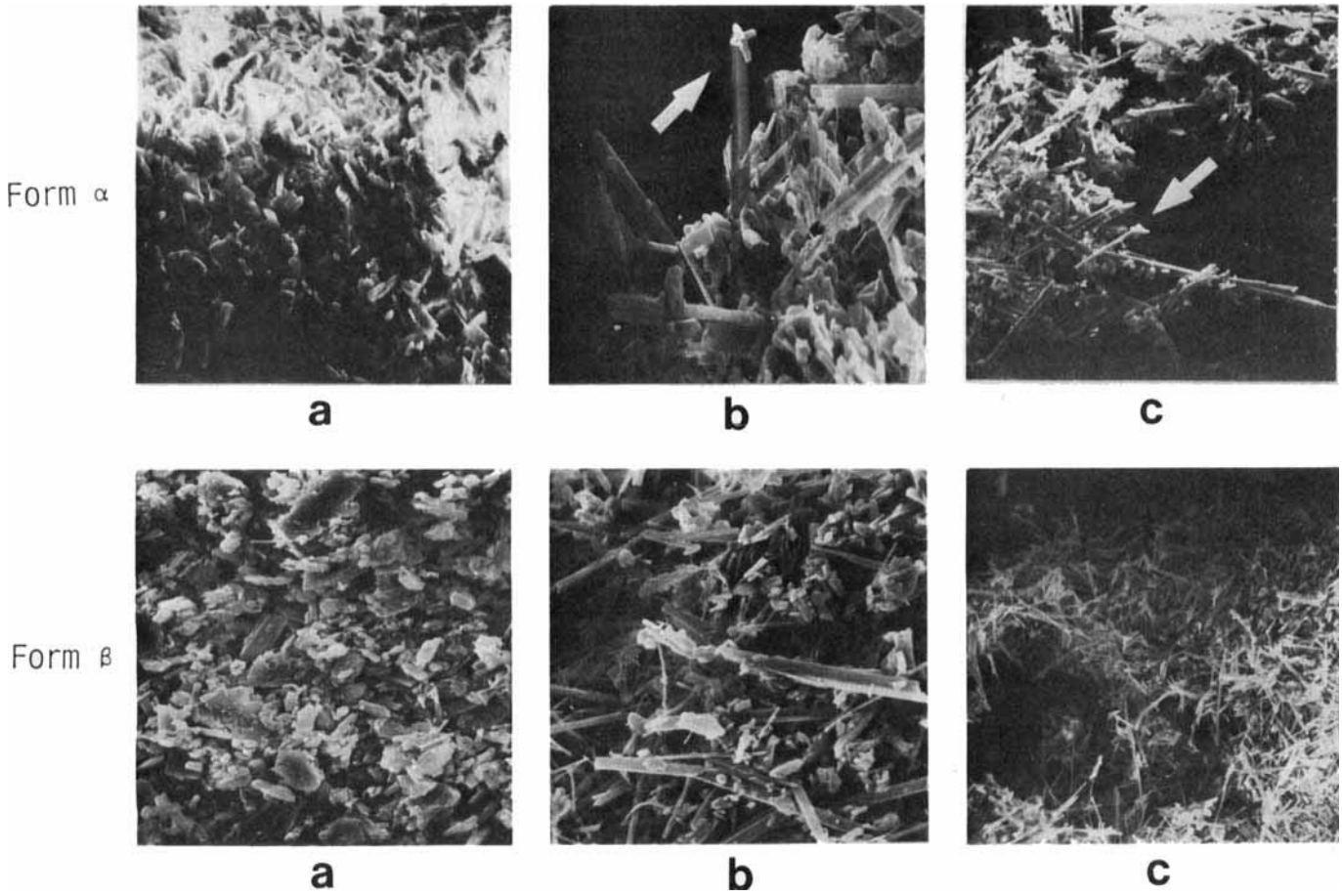

Figure 14—*Scanning electron photomicrographs representing various stages in crystal growth accompanying α → δ and β → δ transformations at 60°C and 80% relative humidity. Key: (a) initial, 2000×, (b) 50% transformed, 2000×; (c) 80% transformed, 600×.*

that prolongation of the induction period led to the subsequent lowering of the rate constant, resulting in further stability. These results indicate that the induction stage is a process that induces control of transformation. The regression analyses showed that these factors were closely correlated with each other at a 5% level of significance. Hence, the following regression equations were obtained:

$$k_1 \times t_i^{0.56} = 0.167 \ (\alpha \rightarrow \delta \text{ transformation}) \qquad \text{(Eq. 5)}$$

$$k_2 \times t_i^{0.88} = 0.319 \ (\beta \rightarrow \delta \text{ transformation}) \qquad \text{(Eq. 6)}$$

It is possible to estimate an approximate induction period for the $\beta \rightarrow \delta$ transformation by substituting the rate constant under a given storage condition (obtained from Fig. 12) into Eq. 6. Assuming that the Arrhenius treatment of the $\alpha \rightarrow \delta$ transformation was applicable in the same temperature range as that of the $\beta \rightarrow \delta$ transformation, the induction period should require not less than ~8.8 years at 25°C.

Microscopic Characterization of Transformation Processes—The morphological changes of the crystal surface in the course of transformation were traced by scanning electron photomicroscopy. Figure 14 shows the photomicrographs of forms α and β which were transformed by 50 and 80% at 60°C and 80% relative humidity in intact samples. Due to minute sizes, any newly born crystal nuclei could not be discriminated in the early stage of transformation. The occurrence and growth of whiskers characterizing form δ were clearly observed during mid and late transformations. The whiskers were thicker and longer in the $\alpha \rightarrow \delta$ transformation than in the $\beta \rightarrow \delta$ transformation. This result may be explained by the fact that the transformation of form α is slower than that of form β, as shown above. Since the transformation rate of form α is independent of moisture, the interface must advance from the nuclei surface into the crystal entity accompanying the growth of the stable form. This view is not contradictory to the previous statement that the growth of the stable phase may be two-dimensional. The knots (arrows in the photos) of sesame seed-sized form α crystals, which are distributed over the surface of acicular crystals of form δ, became thin as the transformation progressed, suggesting their uptake into the crystal entity.

The particle densities of forms α, β, and δ were almost identical, with the measured values being 1.21, 1.21, and 1.19 g/cm^3, respectively. Therefore, it is believed that no visible change in the volume of one crystal occurs during transformation. The fact that acicular crystals much larger than intact crystals in volume are nevertheless growing suggests strongly the sintering of crystals at the potential nuclei formation sites. In this sense, the mechanism of the

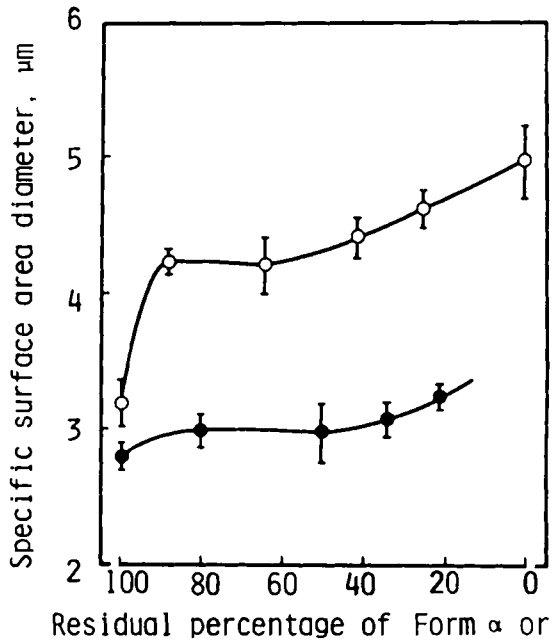

Figure 15—*Changes in particle diameter of samples under transformation. Key: (○) α → δ transformation; (●) β → δ transformation. Each point represents mean ± SD (n = 15).*

present whisker growth is quite different from that of whisker growth on an ethenzamide tablet which is liable to sublimation (29).

The morphological changes were quantitatively confirmed in Fig. 15, in which the specific surface area diameter of the sample was plotted against the percent conversion of form α or β. The growth curves of forms α and β showed a quite similar pattern to the BET-type adsorption isotherm and consisted of three stages: (*a*) a rapidly growing stage up to an ~10% conversion rate; (*b*) a cessation stage without evident increase in particle diameter; (*c*) a regrowing stage of whiskers. The increasing rate of particle diameter of form α at an 80% conversion rate was ~2.8 times as high as that of form β, indicating that a higher increasing rate of the diameter was induced by slower transformation.

In addition to showing the fundamental guideline for solution of a stability problem of polymorphic forms, the practical significance of controlling ambient factors which can maintain the integrity of the selected form has been suggested. A more detailed explanation of the relationship between crystal growth and mechanism of transformation is not available at the present time, and further studies are required to draw definite conclusions.

REFERENCES

(1) M. A. Moustafa, S. A. Khalil, A. R. Ebian, and M. M. Motawi, *J. Pharm. Pharmacol.*, **24,** 921 (1972).

(2) A. R. Ebian, M. A. Moustafa, S. A. Khalil, and M. M. Motawi, *J. Pharm. Pharmacol.*, **25,** 13 (1973).

(3) M. A. Moustafa, S. A. Khalil, A. R. Ebian, and M. M. Motawi, *J. Pharm. Sci.*, **63,** 1103 (1974).

(4) M. A. Moustafa and J. E. Carless, *J. Pharm. Pharmacol.*, **21,** 359 (1969).

(5) E. G. Shami, P. D. Bernardo, E. S. Rattie, and L. J. Ravin, *J. Pharm. Sci.*, **61,** 1318 (1972).

(6) S. Miyazaki, M. Nakano, and T. Arita, *Chem. Pharm. Bull.*, **24,** 1832 (1976).

(7) A. Watanabe, S. Tasaki, Y. Wada, and H. Nakamachi, *Chem. Pharm. Bull.*, **27,** 2751 (1979).

(8) H. Nakamachi, Y. Wada, I. Aoki, Y. Kodama, and K. Kuroda, *Chem. Pharm. Bull.*, **29,** 2956 (1981).

(9) J. Matsunaga, N. Nambu, and T. Nagai, *Chem. Pharm. Bull.*, **24,** 1169 (1976).

(10) H. G. Ibrahim, F. Pisano, and A. Bruno, *J. Pharm. Sci.*, **66,** 669 (1977).

(11) B. W. Müller, *Pharm. Acta Helv.*, **53,** 333 (1978).

(12) A. Chauvet and J. Masse, *Trav. Soc. Pharm. Montpellier*, **38,** 31 (1978).

(13) Y. Matsuda, S. Kawaguchi, H. Kobayashi, and J. Nishijo, *J. Pharm. Pharmacol.*, **32,** 579 (1980).

(14) M. D. Tuladhar, J. E. Carless, and M. P. Summers, *J. Pharm. Pharmacol.*, **35,** 208 (1983).

(15) M. D. Tuladhar, J. E. Carless, and M. P. Summers, *J. Pharm. Pharmacol.*, **35,** 269 (1983).

(16) Y. Matsuda, S. Kawaguchi, H. Kobayashi, and J. Nishijo, *J. Pharm. Sci.*, **73,** 173 (1984).

(17) E. Suito, M. Arakawa, and M. Takahashi, *Kogyokagaku Zasshi*, **59,** 307 (1956).

(18) J. D. Hancock and J. H. Sharp, *J. Am. Ceram. Soc.*, **55,** 74 (1972).

(19 M. Avrami, *J. Chem. Phys.*, **7,** 1103 (1939); B. V. Erofe'ev, *Dokl. Akad. Nauk, SSSR*, **52,** 511 (1946).

(20) H. Schmalzried, in "Solid State Reactions," Verlag Chemie, Weinheim, Federal Republic of Germany, 1981, p. 198.

(21) "Reactions in the Solid State," C. H. Bamford and C. F. H. Tipper, Eds., Elsevier Scientific Publishing Co., Amsterdam, The Netherlands, 1980, pp. 57–86.

(22) "Kagaku Jikken Sohsaho," A. Ogata, T. Koda, and S. Niinobe, Eds., Nankodo Co., Tokyo, 1979, p. 233.

(23) M. C. Ball and L. S. Norwood, *J. Chem. Soc., Ser. A*, **1969,** 1633.

(24) M. C. Ball and R. G. Urie, *J. Chem. Soc., Ser. A*, **1970,** 528.

(25) H. E. Kissinger, *Anal. Chem.*, **29,** 1702 (1957).

(26) S. R. Byrn, in "Solid-State Chemistry of Drugs," Academic, New York, N.Y., 1982, pp. 65–68.

(27) L. F. Jones, D. Dollimore, and T. Nicklin, *Thermochim. Acta*, **13,** 240 (1975).

(28) S. R. Mikhail, D. Dollimore, A. M. Kamel, and N. R. El-Nazer, *J. Appl. Chem. Biotechnol.*, **23,** 419 (1973).

(29) H. Murayama, M. Takahashi, M. Asano, M. Washitake, H. Yuasa, and K. Asahina, *Yakuzaigaku*, **41,** 113 (1981).

ACKNOWLEDGMENTS

This study was presented in part before the 102nd Annual Meeting of the Pharmaceutical Society of Japan, Osaka, April 1982.

The bulk sample of phenylbutazone was generously supplied by Ciba-Geigy (Japan) Ltd. Thanks are also tendered to Dr. H. Nakamachi, Takeda Chemical Industries Ltd., Osaka, for preparation of the scanning electron photomicrographs.